PERGAMON

International Journal of Solids and Structures 40 (2003) 1369–1391

INTERNATIONAL JOURNAL OF SOLIDS and STRUCTURES

www.elsevier.com/locate/ijsolstr

Energy relaxation of non-convex incremental stress potentials in a strain-softening elastic–plastic bar

M. Lambrecht, C. Miehe *, J. Dettmar

Institut für Mechanik (Bauwesen) Lehrstuhl I, Universität Stuttgart, 70550 Stuttgart, Pfaffenwaldring 7, Germany

Received 26 June 2002; received in revised form 24 October 2002

Abstract

We propose a fundamentally new concept to the treatment of material instabilities and localization phenomena based on energy minimization principles in a strain-softening elastic–plastic bar. The basis is a recently developed incremental variational formulation of the local constitutive response for generalized standard media. It provides a quasi-hyperelastic stress potential that is obtained from a local minimization of the incremental energy density with respect to the internal variables. The existence of this variational formulation induces the definition of the material stability of inelastic solids based on convexity properties in analogy to treatments in elasticity. Furthermore, localization phenomena are understood as micro-structure development associated with a non-convex incremental stress potential in analogy to phase decomposition problems in elasticity. For the one-dimensional bar considered the two-phase micro-structure can analytically be resolved by the construction of a sequentially weakly lower semicontinuous energy functional that envelops the not well-posed original problem. This relaxation procedure requires the solution of a local energy minimization problem with two variables which define the one-dimensional micro-structure developing: the volume fraction and the intensity of the micro-bifurcation. The relaxation analysis yields a well-posed boundary-value problem for an objective post-critical localization analysis. The performance of the proposed method is demonstrated for different discretizations of the elastic–plastic bar which document on the mesh-independence of the results.

Keywords: Inelasticity; Material instabilities; Localization; Variational methods; Energy relaxation; Convexification

1. Introduction

Application of standard numerical solution methods to the simulation of localization phenomena in strain-softening elastic–plastic solids typically yields non-objective post-critical results. The reason of this well-known effect is the ill-posedness of the incremental boundary-value problem that demotes a subsequent standard analysis to be physically meaningless. In the context of finite element formulations the crucial mesh-dependence was pointed out for example by Crisfield (1982), de Borst (1987) and Belytschko et al. (1988). A broad spectrum of higher-order theories and associated numerical methods has been

* Corresponding author. Tel.: +49-711-685-6379.
E-mail address: cm@mechbau.uni-stuttgart.de (C. Miehe).

PII: S0020-7683(02)00658-3

developed in the last decades in order to describe in an objective format experimentally observed localized failure mechanisms with highly narrow concentrations of inelastic deformation patterns such as reported in Nadai (1950) and Vardoulakis (1977). These regularization techniques enhance standard theories by introducing different length scale parameters which are often considered to be related to the micro-structure of the material. Representatives are viscoplastic regularization techniques, non-local continuum theories, micro-polar Cosserat theories and the modelling of discontinuities (see for example Needleman, 1988; de Borst and Sluys, 1991; Bažant and Lin, 1988; Mühlhaus and Aifantis, 1991; Larsson et al., 1993; Simó et al., 1993; Miehe and Schröder, 1994). Reviews of this very broad and highly active field of research are provided in Mühlhaus (1995) and de Borst (1987), see also the references cited therein.

In this paper we propose a fundamentally new approach to the treatment of material instabilities and localization phenomena in a strain-softening elastic–plastic bar that bases on the minimization of incremental energies. The concept offers the following two perspectives to a localization analysis. Firstly, statements of the material stability of inelastic solids are based on the convexity condition of incremental energy functions in analogy to treatments in finite elasticity. Secondly, localization phenomena are interpreted as micro-structure developments associated with non-convex incremental energy functions in analogy to elastic phase-decomposition problems. The micro-phases arising can be resolved by the relaxation of non-sequentially weakly lower semicontinuous energy functionals based on the convexification of the incremental stress potential function. The relaxed problem provides a well-posed formulation for an objective analysis of localizations. The framework developed yields a mathematically well-posed alternative to the above mentioned classical techniques.

The setting up of a general incremental variational formulation of inelasticity for the one-dimensional model frame in Section 2 follows closely the recent papers (Miehe, 2002; Miehe et al., 2002) which are conceptually in line with the work of Ortiz and Repetto (1999). It focuses on a general internal variable formulation of inelasticity for generalized standard media governed by only two scalar functions: the energy storage function and the dissipation function. The general set up can be related to the works of Biot (1965), Ziegler (1963), Germain (1973), Halphen and Nguyen (1975), see also the recent treatments (Maugin, 1992; Nguyen, 2000). In Section 2, we lay out a distinct incremental variational formulation for this class of materials. Here, a quasi-hyperelastic stress potential at discrete times is obtained from a local minimization problem of the constitutive response. The underlying basic approach is the determination of a path of internal variables in a finite increment of time that minimizes a generalized incremental work expression. As already pointed out by Martin (1975), such an extremal path induces the existence of a potential for the stress. The minimization path within the time increment under consideration is approximated by a deformation-driven constitutive integration algorithm for the internal variables. The incremental algorithmic parameter associated with this integration scheme is then considered to be the variable of the discretized minimization problem.

Key advantage of the variational formulation outlined is the opportunity to define the stability of the incremental inelastic response in terms of terminologies used in elasticity. It means in particular that classical definitions of localized failure as outlined in Thomas (1961), Hill (1962) and Rice (1976) can be related to the convexity conditions of the above introduced incremental stress potential in analogy to treatments in finite elasticity (see for example Dacorogna, 1989; Krawietz, 1986; Ciarlet, 1988; Marsden and Hughes, 1994; Šilhavý, 1997). Here, a necessary condition for the existence of minimizers forces the energy functions to be sequentially weakly lower semicontinuous. In the scalar case a sufficient condition is the convexity of the stored elastic energy function. This general result was at first obtained by Tonelli (1921) and then generalized by DeGiorgi (1968), Rockafellar (1970), among others. The above outlined variational formulation enables us to extend these results to the incremental response of inelasticity. It is concerned to be stable if the incremental stress potential is convex. A first approach to the definition of material stability based on convexity properties of an incremental stress potential can be found in Runesson and Larsson (1993). Within the framework of a standard dissipative material, they constructed a variational principle and pointed out that in case of strain-softening plasticty the loss of material stability is associated to non-convex incremental energy functions.

As a consequence, we consider localized material response as a phase decay of the homogeneous strain state on the macro-scale into a two-phase micro-structure. With regard to a further analysis of this phenomenon, the incremental variational setting opens up the opportunity to apply the concept of relaxation of non-convex variational problems to inelastic solids. A relaxation is associated with a convexification of the non-convex energy function by constructing its convex envelope. The convexification is concerned with the determination of the micro-structure. We refer to Dacorogna (1989), Müller (1998) for a sound mathematical basis.

The structure of the paper is as follows: As a key basis for the subsequent treatment, in Section 2 a variational formulation of the local constitutive response for normal-dissipative standard materials in presented by defining an incremental stress potential. Section 3 defines the stability of the material response in terms of the convexity of the potential. Section 4 then outlines a relaxation technique for non-convex localized material behavior that determines the evolution of the micro-structure. In Section 5 we comment on the global variational formulation for the incremental boundary-value problem of the inelastic solid. The performance of the relaxation analysis proposed is demonstrated for different discretizations of the elastic–plastic bar which report on the objectivity of the results.

2. Variational formulation of the local constitutive response

The setting up of a general incremental variational formulation of inelasticity for the one-dimensional model frame in this section follows closely the recent papers (Miehe, 2002; Miehe et al., 2002). We adapt the first one to a one-dimensional model frame.

2.1. Internal variable formulation of inelasticity

Let $\varepsilon \in \mathbb{R}$ be the strain governing the homogeneous deformation of a material at time $t \in \mathbb{R}_0^+$. Focusing on purely mechanical problems, the local constitutive response $x \in \mathscr{B}$ is assumed to be physically constrained by the so-called Clausius–Planck inequality for the internal dissipation

$$\mathscr{D} := \sigma\dot{\varepsilon} - \dot{\psi} \geqslant 0, \tag{1}$$

where σ denotes the stress. The local energy storage is governed by an *energy storage function* $\psi : \mathbb{R} \times \mathbb{R} \times \mathbb{R} \rightarrow \mathbb{R}_0^+$ that depends on the strain $\varepsilon \in \mathbb{R}$ and a generalized vector $\mathscr{I} \in \mathbb{R} \times \mathbb{R}$ of internal variables. Insertion into (1) yields the constitutive equation for the stress

$$\sigma = \partial_\varepsilon \psi(\varepsilon, \mathscr{I}) \tag{2}$$

and the reduced dissipation inequality

$$\mathscr{D} = \mathscr{F} \cdot \dot{\mathscr{I}} \geqslant 0 \quad \text{with } \mathscr{F} := -\partial_{\mathscr{I}} \psi(\varepsilon, \mathscr{I}), \tag{3}$$

where $\mathscr{F} \in \mathbb{R} \times \mathbb{R}$ is a generalized vector of internal forces conjugate to the internal variables $\mathscr{I}$. The evolution $\dot{\mathscr{I}}$ of the internal variables is governed by a scalar *dissipation function* $\phi : \mathbb{R} \times \mathbb{R} \rightarrow \mathbb{R}$. This function is assumed to depend on the flux $\dot{\mathscr{I}}$ of the internal variables. Using the definition of the sub-differential, it determines the evolution of $\mathscr{I}$ in time by the constitutive differential equation

$$0 \in \partial_{\mathscr{I}} \psi(\varepsilon, \mathscr{I}) + \partial_{\dot{\mathscr{I}}} \phi(\dot{\mathscr{I}}) \quad \text{with } \mathscr{I}(0) = \mathscr{I}_0 \tag{4}$$

often referred to as Biot's equation of standard dissipative systems (see Biot, 1965; Nguyen, 2000). The two constitutive equations (2) and (4) determine the stress response of a normal dissipative material in a deformation-driven process where the strain ε is prescribed. Based on the definition $(3)_2$ of the internal forces $\mathscr{F}$, one introduces a dual dissipation function ϕ^* depending on the forces by the Legendre–Fenchel transformation (see Rockafellar, 1970)

$$\phi^*(\mathscr{F}) = \sup_{\dot{\mathscr{I}}}\{\mathscr{F}\cdot\dot{\mathscr{I}} - \phi(\dot{\mathscr{I}})\}. \tag{5}$$

The definitions $(3)_2$ and (5) induce the alternative representation

$$\dot{\mathscr{I}} \in \partial_{\mathscr{F}}\phi^*(\mathscr{F}) \tag{6}$$

of Biot's equation $(4)_1$. The internal forces are assumed to be bounded by a convex set $\mathbb{E} \in \mathbb{R}\times\mathbb{R}$. The level set function $f : \mathbb{R}\times\mathbb{R} \to \mathbb{R}_0^+$ with the threshold $c \in \mathbb{R}_0^+$ is assumed to describe the convex domain

$$\mathbb{E} := \{\mathscr{F} | f(\mathscr{F}) \leqslant c\}. \tag{7}$$

The level set function is positively homogeneous of degree one $f(\theta\mathscr{F}) = \theta f(\mathscr{F})$. For a known elastic domain (7) the dissipation function for a rate-independent model of inelasticity may be defined by the classical principle of maximum dissipation. It defines the dissipation function by the constrained maximum problem

$$\phi(\dot{\mathscr{I}}) = \sup_{\mathscr{F}\in\mathbb{E}}\{\mathscr{F}\cdot\dot{\mathscr{I}}\}, \tag{8}$$

that can be solved by the Lagrange formulation

$$\phi(\dot{\mathscr{I}}) = \sup_{\mathscr{F}}\{\mathscr{F}\cdot\dot{\mathscr{I}} - \lambda[f(\mathscr{F}) - c]\}. \tag{9}$$

The Lagrange parameter λ is determined by the Karush–Kuhn–Tucker conditions

$$\lambda \geqslant 0, \quad f \leqslant c, \quad \lambda(f - c) = 0. \tag{10}$$

Observe that (9) may be interpreted as the Legendre–Fenchel transformation of the dual dissipation potential

$$\phi^*(\mathscr{F}) = \lambda[f(\mathscr{F}) - c]. \tag{11}$$

Exploitation of (6) yields the evolution equation for the internal variables

$$\dot{\mathscr{I}} = \lambda\partial_{\mathscr{F}} f(\mathscr{F}). \tag{12}$$

It splits the evolution $\dot{\mathscr{I}}$ of the internal variables into what can be considered as the amount λ and the normal direction $\partial_{\mathscr{F}} f$ of the inelastic flow. Inserting (12) into (9), taking into account the homogeneity of degree one of the level set function and $(10)_3$ yield the simple form of the dissipation function

$$\phi = c\lambda. \tag{13}$$

2.2. Incremental variational formulation of inelasticity

In analogy to Miehe (2002) we discuss an integrated version of constitutive equations giving a consistent approximation of the continuous differential equation (4) in a finite time increment $[t_n, t_{n+1}] \in \mathbb{R}^+$. Key point is the definition of an *incremental stress potential function* W depending on the strain $\varepsilon_{n+1} := \varepsilon(t_{n+1})$ at time t_{n+1} that determines the stress σ_{n+1} at t_{n+1} by the quasi-hyperelastic function evaluation

$$\sigma_{n+1} = \partial_\varepsilon W(\varepsilon_{n+1}). \tag{14}$$

The function W has to cover characteristics of the storage function ψ and the dissipation function ϕ. We consider the variational problem

$$W(\varepsilon_{n+1}) = \inf_{\mathscr{I}} \int_{t_n}^{t_{n+1}} [\dot{\psi} + \phi]\,\mathrm{d}t \quad \text{with } \mathscr{I}(t_n) = \mathscr{I}_n. \tag{15}$$

For a prescribed strain, this problem defines the incremental stress potential function W as a minimum of the generalized work $\int_{t_n}^{t_{n+1}} [\dot{\psi} + \phi]\,\mathrm{d}t$ done on the material in the time increment under consideration. Starting with the given initial condition $\mathscr{I}(t_n) = \mathscr{I}_n$, the minimum problem defines an optimal path of the internal variables $\mathscr{I}(t)$ for $t \in [t_n, t_{n+1}]$, including the right boundary value $\mathscr{I}_{n+1} := \mathscr{I}(t_{n+1})$. For a detailed discussion we refer to Miehe (2002).

2.3. Discrete variational formulation of inelasticity

The numerical formulation of the incremental variational formulation (15) bases on a straightforward discretization of the evolution equation (12) and the dissipation function (13) in the time interval under consideration. At first we consider an algorithm that approximates the integration

$$\mathscr{I}_{n+1} = \mathscr{I}_n + \int_{t_n}^{t_{n+1}} \lambda \partial_{\mathscr{F}} f(\mathscr{F})\,\mathrm{d}t \tag{16}$$

in a deformation-driven scenario where the strain ε_{n+1} of the material is prescribed and considered to be given. We approximate the current internal variables

$$\mathscr{I}_{n+1} = \mathscr{I}_n + \gamma \partial_{\mathscr{F}} f_{n+1} \tag{17}$$

by an algorithm that is viewed only as a function of the algorithmic incremental parameter

$$\gamma := \lambda_{n+1} \Delta t \quad \text{with } \Delta t := t_{n+1} - t_n. \tag{18}$$

Due to $(10)_1$, this algorithmic parameter is constrained by the loading cone

$$\gamma \in \mathscr{K} := \{\gamma \in \mathbb{R} | \gamma \geqslant 0\}. \tag{19}$$

Insertion of the update algorithm (17) for the internal variables and the discrete incremental dissipation $\int_{t_n}^{t_{n+1}} \phi\,\mathrm{d}t = c\gamma$ into the variational principle (15) induces the function

$$W^h(\varepsilon_{n+1}, \gamma) = \psi(\varepsilon_{n+1}, \mathscr{I}_{n+1}(\gamma)) - \psi_n + c\gamma. \tag{20}$$

The discretization of the variational problem (15) then reads

$$W(\varepsilon_{n+1}) = \inf_{\gamma \in \mathscr{K}} W^h(\varepsilon_{n+1}, \gamma). \tag{21}$$

Thus the continuous formulation (15) of the incremental variational formulation is approximated by the formulation (21) that minimizes the function (20) with respect to the algorithmic incremental parameter γ defined in (18). The Karush–Kuhn–Tucker optimality conditions are denoted as

$$W^h_{,\gamma} \geqslant 0, \quad \gamma \geqslant 0, \quad W^h_{,\gamma}\gamma = 0. \tag{22}$$

For the case of inelastic loading $\gamma > 0$, the solution may be obtained by a Newton algorithm

$$\gamma \Leftarrow \gamma - [W^h_{,\gamma\gamma}]^{-1} W^h_{,\gamma}. \tag{23}$$

The iteration is terminated for $|W^h_{,\gamma}| \leqslant \mathrm{tol}$ when the minimizing point γ^* is found. Having solved the discrete incremental variational principle (21), we compute the stress based on a straightforward exploitation of the definitions (14). Taking the derivative of the function (21) with respect to the strain ε_{n+1} at the solution point γ^*, due to the necessary condition $(22)_3$ we get the representation of the stress

$$\sigma_{n+1} = W^h_{,\varepsilon}. \tag{24}$$

Table 1
Solution algorithm for the incremental minimization problem

1. Initialize internal variables $\mathscr{I} = \mathscr{I}_n$ and $\gamma = 0$
2. If $W^h_{,\gamma} > -\text{tol}$ set potential, stress and tangent modulus $W = \psi - \psi_n$, $\sigma_{n+1} = \psi_{,\varepsilon}$, $\mathbb{C}_{n+1} = \psi_{,\varepsilon\varepsilon}$
3. Update internal variables $\mathscr{I} = \mathscr{I}_n + \gamma \partial_{\mathscr{F}} f_{n+1}$
4. Compute derivatives $W^h_{,\gamma}$ and $W^h_{,\gamma\gamma}$ and check tolerance. If $\lvert W^h_{,\gamma}\rvert < \text{tol}$ go to 6
5. Update incremental plastic multiplier $\gamma \Leftarrow \gamma - [W^h_{,\gamma\gamma}]^{-1} W^h_{,\gamma}$ and go to 3
6. Calculate potential, stress and tangent modulus for solution point γ^* $W = W^h$, $\sigma_{n+1} = W^h_{,\varepsilon}$, $\mathbb{C}_{n+1} = W^h_{,\varepsilon\varepsilon} - W^h_{,\varepsilon\gamma}[W^h_{,\gamma\gamma}]^{-1} W^h_{,\gamma\varepsilon}$

The sensitivity of the stress with respect to the strain is governed by the algorithmic tangent modulus

$$\mathbb{C}_{n+1} := \partial^2_{\varepsilon\varepsilon} W(\varepsilon_{n+1}) \tag{25}$$

of the material at time t_{n+1}. Application of the chain rule and the implicit function theorem finally specifies the definition (25) of the modulus as

$$\mathbb{C}_{n+1} := W^h_{,\varepsilon\varepsilon} - W^h_{,\varepsilon\gamma}[W^h_{,\gamma\gamma}]^{-1} W^h_{,\gamma\varepsilon}. \tag{26}$$

Observe that the modulus consists of an elastic contribution and a softening part. The latter is the consequence of the internal degrees of the material represented by a change of the internal variables within the time step under consideration. The solution algorithm for the incremental minimization problem is summarized in Table 1.

3. Stability of the incremental local constitutive response

The incremental variational formulation outlined above for inelastic solids provides a perspective for distinctive computational treatments of material instabilities based on weak convexity notions. Existence results for boundary-value problems of finite elasticity are reviewed in Dacorogna (1989), Krawietz (1986), Müller (1998) and Šilhavý (1997). The introduction of the stress potential W in (21) allows an application of these results to boundary-value problems of the incremental setting of inelasticity. This is achieved by applying statements on the weak convexity such as poly-convexity, quasi-convexity and rank-1-convexity of the storage function ψ of elasticity to the incremental stress potential W of inelasticity. For the one-dimensional problem under consideration the conditions of poly-convexity, quasi-convexity and rank-1-convexity coincide with the convexity condition (see Dacorogna, 1989, and the references cited therein).

3.1. Reformulation of the classical convexity condition

As already mentioned, the existence of regular minimizers is ensured if the potential W is a convex function with respect to the actual strain ε_{n+1}. This general result was at first obtained by Tonelli (1921) and then generalized by DeGiorgi (1968) and Rockafellar (1970), among others. The classical convexity condition reads

$$W(\xi\varepsilon^+ + (1-\xi)\varepsilon^-) \leqslant \xi W(\varepsilon^+) + (1-\xi) W(\varepsilon^-) \tag{27}$$

in terms of the fraction $0 \leqslant \xi \leqslant 1$ and for all admissible strains $\varepsilon^+ \in \mathbb{R}$, $\varepsilon^- \in \mathbb{R}$. Convexity ensures the internal part of the functional (57) to be sequentially weakly lower semicontinuous (s.w.l.s.) (see Dacorogna, 1989)

$$W \text{ convex} \Longleftrightarrow I(u_{n+1}) = \int_{\mathscr{B}} W(\varepsilon_{n+1})\,\mathrm{d}V \text{ s.w.l.s.} \tag{28}$$

This is considered to be the essential property for the existence of sufficiently regular minimizers of the variational problem (57). For further details of existence theorems in elasticity we refer to Ciarlet (1988), Dacorogna (1989), Marsden and Hughes (1994), Šilhavý (1997) and the references cited therein. The classical convexity inequality (27) represents a superordinate criterion that requires the convexity of the reduced incremental potential function in the whole domain of definition. However, the incremental stress potential W may consist of convex and non-convex ranges. In order to detect whether W is convex for a given strain ε_{n+1} we consider the actual strain ε_{n+1} to be described by an interpolation between two strains ε^+ and ε^-

$$\varepsilon_{n+1} := \xi\varepsilon^+ + (1-\xi)\varepsilon^-. \tag{29}$$

Eq. (29) can also be regarded as a compatibility condition that needs to be satisfied by the strains ε^+ and ε^-. For the one-dimensional problem under consideration we introduce the appropriate ansatz

$$\varepsilon^- := \varepsilon_{n+1} - \xi d \quad \text{and} \quad \varepsilon^+ := \varepsilon_{n+1} + (1-\xi)d \tag{30}$$

that parametrizes ε^+ and ε^- in terms of the variables ξ and d. For the sake of brevity in what follows we summarize these two variables in the vector

$$\boldsymbol{c} = [\xi, d]^{\mathrm{T}}. \tag{31}$$

The variable d is denoted as the intensity d of the micro-bifurcation and ξ as the volume fraction of the phase (+). Note that these variables are restricted to be elements of the domain

$$\mathscr{C} := \{\boldsymbol{c} | 0 \leqslant \xi \leqslant 1,\ d \geqslant 0\}. \tag{32}$$

Insertion of (29) and (30) into the right part of the classical convexity inequality (27) yields the minimization function

$$\overline{W}^h(\varepsilon_{n+1}, \boldsymbol{c}) = \xi W(\varepsilon^+) + (1-\xi)W(\varepsilon^-). \tag{33}$$

The definition (33) induces a reformulation of the classical convexity condition (27). The strain ε_{n+1} is a convex point of the incremental stress potential W, if the minimum of the function $\overline{W}^h(\varepsilon_{n+1})$ with respect to the variables ξ and d equals the potential $W(\varepsilon_{n+1})$

$$W(\varepsilon_{n+1}) = \inf_{\boldsymbol{c}\in\mathscr{C}}\{\overline{W}^h(\varepsilon_{n+1}, \boldsymbol{c})\}. \tag{34}$$

Depending on whether condition (34) is satisfied, the strain ε_{n+1} lies in a convex or in a non-convex range of the incremental potential function W. Obviously, the alternative convexity condition (34) is only fulfilled if the minimizing variables are $\xi \in \{0, 1\}$ or $d = 0$. In these cases one or both micro-strains ε^+ or ε^- are identical to the macroscopic strain ε_{n+1}.

3.2. Accompanying check of the convexity condition

The check of convexity condition (34) requires the solution of a non-linear optimization problem in order to detect the minimizing variables $\boldsymbol{c}^* = [\xi^*, d^*]^{\mathrm{T}}$. To avoid the expensive solution of (34), we consider an equivalent convexity inequality by determination of the Gâteaux derivative

$$\frac{\mathrm{d}}{\mathrm{d}\xi}[W(\xi\varepsilon^+ + (1-\xi)\varepsilon^-)]_{\xi=0} \leqslant \frac{\mathrm{d}}{\mathrm{d}\xi}[\xi W(\varepsilon^+) + (1-\xi)W(\varepsilon^-)]_{\xi=0} \tag{35}$$

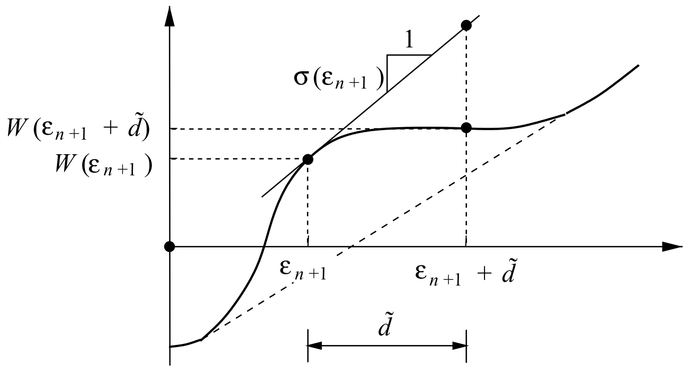

Fig. 1. Weierstrass inequality. For a given actual strain ε_{n+1} the incremental stress potential $W(\varepsilon_{n+1}+\tilde{d})$ is smaller than the extrapolated value $W(\varepsilon_{n+1})+\tilde{d}\sigma(\varepsilon_{n+1})$. As a consequence, the strain ε_{n+1} is not a point of convexity.

of the classical convexity condition (27) with respect to the volume fraction ξ. Taking into account the ansatz (30) for the micro-strains ε^+ and ε^-, we end up with the so-called Weierstrass inequality

$$W(\varepsilon_{n+1})+\tilde{d}\sigma(\varepsilon_{n+1})\leqslant W(\varepsilon_{n+1}+\tilde{d}), \tag{36}$$

with $\tilde{d}\in\mathbb{R}_0^+$. Fig. 1 shows an application of the Weierstrass inequality to a non-convex incremental stress potential W at ε_{n+1}. The incremental stress potential $W(\varepsilon_{n+1}+\tilde{d})$ has to be smaller than the extrapolated value $W(\varepsilon_{n+1})+\tilde{d}\sigma(\varepsilon_{n+1})$. Note that it is not sufficient to check the so-called infinitesimal convexity of $W(\varepsilon_{n+1})$ that is related to the positive second derivative $W_{,\varepsilon\varepsilon}(\varepsilon_{n+1})$. Even if the second derivative was positive, the convexity inequality (34) might not be satisfied (see Figs. 1 and 2). Based on (36) the accompanying check of the convexity condition is performed in the sense

$$W(\varepsilon_{n+1}+\tilde{d})-\tilde{d}\sigma(\varepsilon_{n+1})\begin{cases}\geqslant W(\varepsilon_{n+1}): & \varepsilon_{n+1}\text{ is a convex point}\\ < W(\varepsilon_{n+1}): & \varepsilon_{n+1}\text{ is } \textit{not} \text{ a convex point}\end{cases} \tag{37}$$

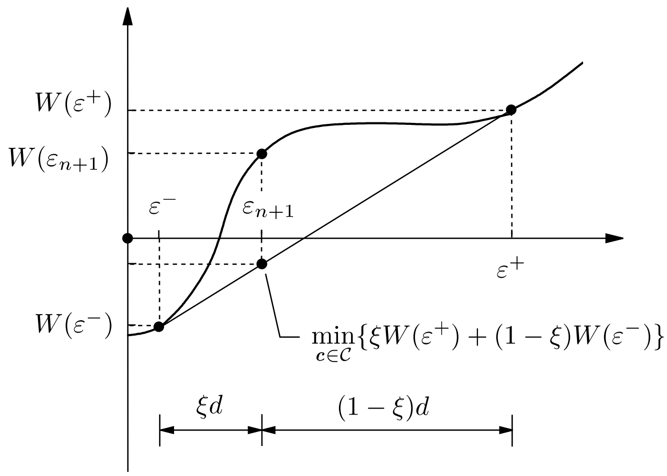

Fig. 2. Convexity of the stress potential. For a given actual strain ε_{n+1} the value of the incremental stress potential W is greater than the minimizing combination of the potentials $W(\varepsilon^+)$ and $W(\varepsilon^-)$ in the corresponding micro-phases. As a consequence, the convexity condition (34) is not satisfied and the incremental potential W is not convex.

for some $\tilde{d}$. If the accompanying evaluation of (36) indicates the loss of convexity, a phase decomposition of the macroscopic strain ε_{n+1} into the two micro-strains ε^+ and ε^- occurs. According to (34), the micro-strains which minimize the volume average $\overline{W}^h$ of the potentials are described by the variables $\boldsymbol{c}^* = [\xi^*, d^*]^{\mathrm{T}}$.

3.3. Mechanical interpretation of convexity

In the context of phase transitions the convexity condition (34) allows an instructive mechanical interpretation: According to (29) the strain ε_{n+1} can be regarded as a homogenization of the two strains ε^- and ε^+. The reformulated convexity condition (34) says that the homogeneous deformation state ε_{n+1} is stable as long as no combination of two phases (+) and (−) exists that possesses a lower energetic level

$$\xi W(\varepsilon^+) + (1-\xi) W(\varepsilon^-) < W(\varepsilon_{n+1}). \tag{38}$$

Fig. 2 shows the shape of a non-convex incremental stress potential W. Obviously, the incremental potential $W(\varepsilon_{n+1})$ is greater than the interpolation of the incremental potentials $W(\varepsilon^+)$ and $W(\varepsilon^-)$ corresponding to the two phases (+) and (−). As a consequence, the homogeneous deformation state is not stable and decomposes into the micro-strains ε^+ and ε^-. These two strains described in terms of the ansatz (30) minimize the function $\overline{W}^h$ with respect to the intensity d and the volume fraction ξ.

4. Relaxation of the non-convex constitutive response

Key advantage of the variational formulation for the constitutive response is the opportunity to apply the concept of relaxation of non-convex variational problems to strain-softening inelastic solids. In the case of a non-convex incremental potential W, an energy minimizing micro-structure develops. A relaxation is associated with a convexification of the non-convex function W by constructing its convex envelope W_{C} as discussed below. The convexification is concerned with the determination of a micro-structure arising. We refer to Dacorogna (1989), Šilhavý (1997) and Müller (1998) for a sound mathematical basis. In this section we present, based on the general concept of relaxation, a comprehensive approach to the treatment of localization.

4.1. Convexification of the incremental potential

If the incremental potential function $W(\varepsilon_{n+1})$ is not convex in the sense of (36), the functional I defined in (28) is not sequentially lower semicontinuous. As a consequence, the minimum of the incremental boundary-value problem (57) is not attained. Following Dacorogna (1989) we consider a relaxed functional

$$I_{\mathrm{C}}(u_{n+1}) = \int_{\mathscr{B}} W_{\mathrm{C}}(\varepsilon_{n+1})\,\mathrm{d}V, \tag{39}$$

where the non-convex integrand W is replaced by its convex envelope W_{C}. The convexified function

$$W_{\mathrm{C}}(\varepsilon_{n+1}) = \inf_{\boldsymbol{c}\in\mathscr{C}} \{\overline{W}^h(\varepsilon_{n+1}, \boldsymbol{c})\} \tag{40}$$

is defined by the above discussed minimization problem that appears in the convexity condition (34). The convexified potential is identical to $\overline{W}^h(\varepsilon_{n+1}, \boldsymbol{c}^*)$ which characterizes the volume average of the potentials in the micro-phases (+) and (−). The first and second derivatives of the convexified function define the relaxed stress and the tangent modulus

$$\bar{\sigma}_{n+1} := \partial_\varepsilon W_{\mathrm{C}}(\varepsilon_{n+1}) \quad \text{and} \quad \overline{\mathbb{C}}_{n+1} := \partial^2_{\varepsilon\varepsilon} W_{\mathrm{C}}(\varepsilon_{n+1}). \tag{41}$$

The crucial point of the convexification analysis lies in the solution of the optimization problem (40) that yields the variables $\boldsymbol{c}^* = [\xi^*, d^*]^{\mathrm{T}}$ characterizing the micro-strains ε^+ and ε^-.

4.2. Numerical solution of the minimization problem of relaxation

In this section we comment on the numerical solution of the minimization problem (40). If the Weierstrass inequality (36) is not satisfied, two variables $0 < \xi^* < 1$ and $d^* > 0$ exist which minimize the function $\overline{W}^h$ defined in (33). The necessary condition of the minimization problem is

$$\overline{W}^h_{,\boldsymbol{c}} = \mathbf{0}. \tag{42}$$

As the minimizing function $\overline{W}^h$ is non-convex with respect to $\boldsymbol{c}$, a standard Newton iteration scheme for arbitrary initial values cannot be applied. We will comment on this peculiarity in Section 6. Therefore, we at first discretize the admissible range of the volume fraction and the intensity of the micro-bifurcation and filter out the minimum

$$\boldsymbol{c}^*_{ij} = \arg\{\min_{\boldsymbol{c}_{ij}\in\mathscr{C}}\{\overline{W}_h(\varepsilon_{n+1}, \boldsymbol{c}_{ij})\}\} \quad \text{with } \boldsymbol{c}_{ij} = [i\Delta\xi, j\Delta d]^{\mathrm{T}} \tag{43}$$

for given increments $\Delta\xi \in \mathbb{R}^+$, $\Delta d \in \mathbb{R}^+$ and $i \in \mathbb{N}$, $j \in \mathbb{N}$. The discrete minimizing combination then serves as a starting value $\boldsymbol{c}^*_{ij}$ for the Newton update scheme

$$\boldsymbol{c} \Leftarrow \boldsymbol{c} - [\overline{W}^h_{,\boldsymbol{cc}}]^{-1}[\overline{W}^h_{,\boldsymbol{c}}]. \tag{44}$$

The Newton iteration is terminated for

$$\|\overline{W}^h_{,\boldsymbol{c}}(\varepsilon_{n+1}, \boldsymbol{c}^*)\| < \text{tol}, \tag{45}$$

when $\boldsymbol{c}^*$ is considered to be the solution of (40). The algorithm for the numerical solution of the minimization problem of the convexification analysis is summarized in Table 2.

4.3. Numerical computation of the relaxed stress and tangent modulus

The relaxed stress and the tangent modulus are obtained by straightforward evaluation of the derivatives (41) of the convexified stress potential (40). The first derivative of (40) with respect to the strain ε_{n+1} at the solution point $\boldsymbol{c}^*$ reads

$$\partial_\varepsilon W_{\mathrm{C}} = \overline{W}^h_{,\varepsilon} + [\overline{W}^h_{,\boldsymbol{c}}][\boldsymbol{c}_{,\varepsilon}]. \tag{46}$$

The last term vanishes due to the necessary condition (42) of the minimization problem. Thus we identify the relaxed stress

$$\bar{\sigma}_{n+1} = \overline{W}^h_{,\varepsilon}. \tag{47}$$

Table 2
Solution algorithm for the minimization problem of convexification

1. For a pattern of combinations $\boldsymbol{c}_{ij} = [i\Delta\xi, j\Delta d]^{\mathrm{T}}$ filter out the minimum $\boldsymbol{c}^*_{ij} = \arg\{\min_{\boldsymbol{c}_{ij}\in\mathscr{C}}\{\overline{W}^h(\varepsilon_{n+1}, \boldsymbol{c}_{ij})\}\}$
2. For the initial value $\boldsymbol{c}^*_{ij}$ initialize Newton scheme $\boldsymbol{c} \Leftarrow \boldsymbol{c} - [\overline{W}^h_{,\boldsymbol{cc}}(\varepsilon_{n+1}, \boldsymbol{c})]^{-1}\overline{W}^h_{,\boldsymbol{c}}(\varepsilon_{n+1}, \boldsymbol{c})$ that is terminated if $\lvert\overline{W}^h_{,\boldsymbol{c}^*}\rvert < \text{tol}$ when $\boldsymbol{c}^*$ is considered to be the solution point

The second derivative of the convexified incremental stress potential reads

$$\partial^2_{\varepsilon\varepsilon} W_C = \overline{W}^h_{,\varepsilon\varepsilon} + [\overline{W}^h_{,\varepsilon \boldsymbol{c}}][\boldsymbol{c}_{,\varepsilon}]. \tag{48}$$

The sensitivity of $\boldsymbol{c}$ with respect to the macro-strain is obtained by taking the linearization of (42) yielding the expression

$$\boldsymbol{c}_{,\varepsilon} = -[\overline{W}^h_{,\boldsymbol{cc}}]^{-1}[\overline{W}^h_{,\boldsymbol{c}\varepsilon}]. \tag{49}$$

Insertion into (48) finally specifies the definition $(41)_2$ of the relaxed tangent modulus as

$$\overline{\mathbb{C}}_{n+1} = \overline{W}^h_{,\varepsilon\varepsilon} - [\overline{W}^h_{,\varepsilon \boldsymbol{c}}][\overline{W}^h_{,\boldsymbol{cc}}]^{-1}[\overline{W}^h_{,\boldsymbol{c}\varepsilon}]. \tag{50}$$

Observe that the macro-modulus consists of the volume average of the micro-moduli and a softening part. The latter is the consequence of the development of the micro-phases. The derivatives of the minimizing function $\overline{W}^h$ needed in the above outlined treatments are summarized in Appendix A.

4.4. Mechanical interpretation of convexification

4.4.1. Relaxed stress and tangent modulus

The loss of convexity of the stress potential W indicates the loss of stability of the homogeneous deformation state ε_{n+1} and initializes the development of micro-structures. The volume average $\xi\varepsilon^+ + (1-\xi)\varepsilon^-$ of the micro-strains coincides with the homogeneous strain ε_{n+1}. The form of the micro-phases is such that they minimize the homogenized incremental work

$$W_C(\varepsilon_{n+1}) = \min_{\varepsilon^+,\varepsilon^-}\{\xi W(\varepsilon^+) + (1-\xi)W(\varepsilon^-)\} \tag{51}$$

with respect to the intensity d of the micro-bifurcation and the volume fraction ξ. The variable ξ can be understood as a probability measure in the sense of Young (1921) (see also Carstensen and Roubíček, 2000). The necessary conditions for the solution of the above minimization problem read

$$\left.\begin{aligned} \overline{W}^h_{,d} &= \xi(1-\xi)[\sigma(\varepsilon^+) - \sigma(\varepsilon^-)] = 0, \\ \overline{W}^h_{,\xi} &= W(\varepsilon^+) - W(\varepsilon^-) - d[\xi\sigma(\varepsilon^+) + (1-\xi)\sigma(\varepsilon^-)] = 0. \end{aligned}\right\} \tag{52}$$

The first condition $(52)_1$ states that the stresses in the micro-phases (+) and (−) are in equilibrium. This allows the conclusion from $(52)_2$ that the slope of the convex envelope is constant and identical to the micro-stress. Some algebraic manipulations confirm that the relaxed tangent modulus equals zero

$$\bar{\sigma}_{n+1} = \sigma(\varepsilon^+) = \sigma(\varepsilon^-) \quad \text{and} \quad \overline{\mathbb{C}}_{n+1} = 0. \tag{53}$$

Fig. 3 depicts the shape of a non-convex potential function and its convex envelope that is described by the micro-strains ε^- and ε^+ in terms of the volume fraction ξ^* and the micro-shearing d^*. In the non-convex range $\varepsilon^- < \varepsilon_{n+1} < \varepsilon^+$ the non-convex incremental potential function W is replaced by its convex envelope W_C. The necessary conditions (52) uniquely characterize the shape of the convex envelope W_C as depicted in Fig. 3. The convexified incremental potential $W_C(\varepsilon_{n+1})$ is obtained by a fictitious projection of the non-convex incremental potential $W(\varepsilon_{n+1})$ onto the convex envelope. As a consequence, the convexification analysis yields a perfectly plastic stress response in the increment considered. As plotted in Fig. 4, the relaxed stress $\bar{\sigma}_{n+1}$ at ε_{n+1} is associated with a Maxwell-type line similar to classical treatments in phase-decompositions of real gases (see e.g. Rowlinson, 1958; Krawietz, 1986; Dacorogna, 1989).

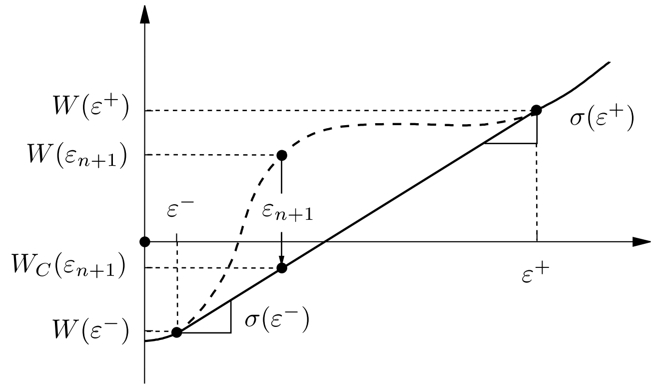

Fig. 3. Convexification of a non-convex stress potential. At ε_{n+1} the incremental stress potential W is not convex (- - -). As a consequence, the macroscopic deformation state ε_{n+1} is not stable and decomposes into two micro-phases (+) and (−) which describe the convex envelope (—).

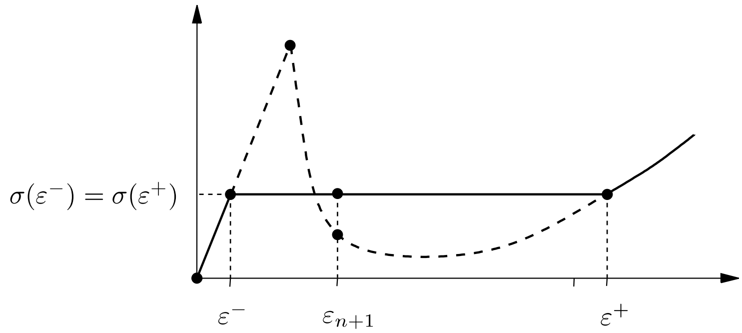

Fig. 4. Convexification of a non-convex stress potential. Due to the constant slope of the convex envelope W_C the relaxed stress $\bar{\sigma}_{n+1}$ is constant in the non-convex range. As a consequence, the convexification of the non-convex incremental stress potential (- - -) leads to an incrementally perfectly plastic response (—).

4.4.2. Transition to the next time increment

As pointed out above the convexification analysis represents a two-scale homogenization analysis of two micro-phases (+) and (−) which arise because of an instability of the homogeneous deformation state. As a consequence, in each phase different internal variables $\mathscr{I}^+$ and $\mathscr{I}^-$ emerge. After the transition to the next time increment the constitutive response at the beginning of the new increment must coincide to that at the end of the previous increment. This trivial statement induces the separate update of the internal variables for each phase

$$\mathscr{I}_n^+ \Leftarrow \mathscr{I}^+ \quad \text{and} \quad \mathscr{I}_n^- \Leftarrow \mathscr{I}^-. \tag{54}$$

Furthermore, for the limiting case $\varepsilon_{n+1} \to \varepsilon_n$ the consistency condition $(52)_2$ must be satisfied for the previous constitutive variables, i.e. $\overline{W}^h_{,\xi} = W(\varepsilon_n^+) - W(\varepsilon_n^-) - d_n\bar{\sigma}_n = 0$. In contrast to the original definition (20) of the incremental stress potential we then have to consider the alternative definitions

$$\left.\begin{aligned} W^h(\varepsilon^+,\gamma) &= \psi(\varepsilon^+,\mathscr{I}^+(\gamma)) - \psi_n(\varepsilon_n^+,\mathscr{I}_n^+) + c\gamma + d_n\bar{\sigma}_n, \\ W^h(\varepsilon^-,\gamma) &= \psi(\varepsilon^-,\mathscr{I}^-(\gamma)) - \psi_n(\varepsilon_n^-,\mathscr{I}_n^-) + c\gamma \end{aligned}\right\} \tag{55}$$

of the potentials in the micro-phases (+) and (−).

Table 3
Algorithm of the two-phase relaxation procedure

1. Homogeneous analysis Solve incremental minimization problem $W(\varepsilon_{n+1}) = \min_\gamma\{W^h(\varepsilon_{n+1},\gamma)\}$ and compute stress and tangent modulus $\sigma_{n+1} = \partial_\varepsilon W(\varepsilon_{n+1})$ and $\mathbb{C}_{n+1} = \partial^2_{\varepsilon\varepsilon} W(\varepsilon_{n+1})$
2. Loss of material stability Check convexity of incremental stress potential with Weierstrass inequality $W(\varepsilon_{n+1}) + \tilde{d}\sigma(\varepsilon_{n+1}) - W(\varepsilon_{n+1} + \tilde{d}) \leqslant -\text{tol}$ If $W(\varepsilon_{n+1})$ is convex update internal variables $\mathscr{I}_n \Leftarrow \mathscr{I}$ and continue to the next time increment with 1, else go to 3
3. Two-phase relaxation analysis Solve minimization problem $W_C(\varepsilon_{n+1}) = \min_c\{\overline{W}^h(\varepsilon_{n+1},\boldsymbol{c})\}$ of convexification and compute relaxed stress and tangent modulus $\bar{\sigma}_{n+1} = \partial_\varepsilon W_C(\varepsilon_{n+1})$ and $\overline{\mathbb{C}}_{n+1} = \partial^2_{\varepsilon\varepsilon} W_C(\varepsilon_{n+1})$
4. Recovery of material stability Check if volume fraction equals zero or one $\xi < \text{tol}$ or $\xi > 1 - \text{tol}$ If necessary, update homogeneous internal variables $\mathscr{I}_n \Leftarrow \mathscr{I}^-$ or $\mathscr{I}_n \Leftarrow \mathscr{I}^+$, respectively, and continue to the next time increment with 1. Otherwise perform update $\mathscr{I}^+_n \Leftarrow \mathscr{I}^+$, $\mathscr{I}^-_n \Leftarrow \mathscr{I}^-$ for each phase separately and continue with 3

4.4.3. Recovery of the stable homogeneous state

If the volume fraction ξ becomes zero or one, only one phase is still present, i.e. $\varepsilon^- = \varepsilon_{n+1}$ or $\varepsilon^+ = \varepsilon_{n+1}$. This can be interpreted as the recovery of a stable homogeneous state. Accordingly, we perform the update of the homogeneous internal variables

$$\mathscr{I}_n = \mathscr{I}^- \text{ if } \xi < \text{tol} \quad \text{or} \quad \mathscr{I}_n = \mathscr{I}^+ \text{ if } \xi > 1 - \text{tol} \tag{56}$$

and continue with the homogeneous analysis including the accompanying check of convexity outlined in Section 3.2. The scheme of the two-phase relaxation procedure is summarized in Table 3.

5. Global incremental variational problem

Based on the variational formulation of the local constitutive response outlined in Section 2, we consider the subsequent energetic formulation of the incremental boundary-value problem of inelasticity.

5.1. Incremental variational formulation of the convex response

Let $u : \mathscr{B} \times \mathbb{R} \to \mathbb{R}$ denote the displacement field of a continuum $\mathscr{B} \subset \mathbb{R}$ at a material point $x \in \mathscr{B}$ and time $t \in \mathbb{R}$. Then $\varepsilon = u'$ is the strain. The incremental potential energy of the elastic–plastic continuum associated with the increment $[t_n, t_{n+1}]$ is a function of the displacement field u and has the form

$$\Pi(u_{n+1}) = \int_{\mathscr{B}} [W(\varepsilon_{n+1}) - u_{n+1}\tilde{\gamma}_{n+1}]\,\mathrm{d}V - \int_{\partial\mathscr{B}_t} u_{n+1}\tilde{\sigma}_{n+1}\,\mathrm{d}A. \tag{57}$$

W is the incremental stress potential function defined in (15), their first and second derivatives are the current stress and tangent modulus defined in (24) and (25), respectively. $\tilde{\gamma}(x,t)$ denotes a given body force field at $x \in \mathscr{B}$ and $\tilde{\sigma}(x,t)$ a given stress field at $x \in \partial\mathscr{B}_t$ on the boundary. As usual, we consider a decomposition of the surface into a part where the deformation is prescribed and a part where the tractions are given, i.e. $\partial\mathscr{B} = \partial\mathscr{B}_u \cup \partial\mathscr{B}_t$ and $\partial\mathscr{B}_u \cap \partial\mathscr{B}_t = \emptyset$. The current displacement field of the inelastic solid is then determined by the incremental variational principle

$$\Pi(u^*_{n+1}) = \inf_{u_{n+1}\in\mathscr{U}} \Pi(u_{n+1}) \tag{58}$$

that minimizes the incremental potential energy for an admissible displacement field

$$u \in \mathscr{U} := \{u | u = \tilde{u}(x) \text{ on } \partial\mathscr{B}_u\} \tag{59}$$

associated with prescribed deformations $\tilde{u}$ at $x \in \partial\mathscr{B}_u$ on the boundary.

5.2. Incremental variational formulation of the non-convex response

For the case when material instabilities are detected at a point $x \in \mathscr{B}$ we face a non-convexity of the incremental potential W in some region of the inelastic solid. Then the existence of solutions of (58) is not ensured, because property (34) is lost. Based on the treatment outlined in Section 4 we then consider a relaxation of the functional (58)

$$\Pi_C(u_{n+1}) = \int_{\mathscr{B}} [W_C(\varepsilon_{n+1}) - u_{n+1}\tilde{\gamma}_{n+1}] \, dV - \int_{\mathscr{B}_t} u_{n+1}\tilde{\sigma}_{n+1} \, dA \tag{60}$$

by replacing the incremental potential W by its convexified counterpart W_C defined in (40). Its first and second derivatives are the current stress $\bar{\sigma}_{n+1}$ and the tangent modulus $\overline{\mathbb{C}}_{n+1}$ defined in (41), they may be considered to be homogenized quantities of the developing micro-structure. The current displacement field of the elastic–plastic solid is then determined by the relaxed incremental variational principle

$$\Pi_C(u^*_{n+1}) = \inf_{u_{n+1} \in \mathscr{U}} \Pi_C(u_{n+1}) \tag{61}$$

that minimizes the relaxed incremental potential energy for the admissible displacement field defined in (59). The relaxed problem (61) is considered to be the well-posed form of the ill-posed problem (58).

6. Numerical examples

We demonstrate the performance of the above outlined relaxation technique by a numerical example that is concerned with the computation of the convexified incremental stress response and the objective simulation of localized failure of a bar in tension. We apply a classical form of rate-independent elasto-plasticity that incorporates strain-softening.

6.1. Variational formulation of the elastoplasticity model

For the elastoplastic model-problem under consideration the internal variables and the dual internal forces have the specific form

$$\mathscr{I} := [\varepsilon^p, A]^T \quad \text{and} \quad \mathscr{F} := [\sigma^p, B]^T, \tag{62}$$

where ε^p denotes the plastic strain and A a scalar internal variable for the description of the strain-softening. σ^p and B are the dual stress-like variables defined in $(3)_2$. The model problem is completed by the definition of the fundamental constitutive functions ψ and f for the strain energy and the level set of the elastic domain, respectively. The elastic response is governed by the strain energy

$$\psi(\varepsilon, \mathscr{I}) = \tfrac{1}{2}E(\varepsilon - \varepsilon^p)^2 + \zeta[A + \eta \exp(-A/\eta)] + \tfrac{1}{2}hA^2. \tag{63}$$

Here, $E \in \mathbb{R}^+$ denotes the elasticity modulus and $\zeta \in \mathbb{R}$, $\eta \in \mathbb{R}$, $h \in \mathbb{R}$ are softening and hardening parameters, respectively. The elastic strain is defined by the difference between the total and the plastic strain $\varepsilon^e = \varepsilon - \varepsilon^p$. Exploitation of (2) yields the stress

$$\sigma = E(\varepsilon - \varepsilon^p). \tag{64}$$

Evaluation of the definition $(3)_2$ leads to the expressions for the thermodynamical internal forces

$$\sigma^{\mathrm{p}} = E(\varepsilon - \varepsilon^{\mathrm{p}}) \quad \text{and} \quad B = -\zeta[1 - \exp(-A/\eta)] - hA. \tag{65}$$

Obviously, σ and σ^{p} are identical because of the additive split of ε into an elastic and a plastic part. We consider a level set function of the form

$$f(\mathscr{F}) = |\sigma| + B. \tag{66}$$

As a consequence of the definition (66) the normal direction has the simple representation

$$\partial_{\mathscr{F}} f = [n, 1]^{\mathrm{T}} \quad \text{with } n := \sigma/|\sigma|. \tag{67}$$

In what follows we evaluate the discrete variational formulation of inelasticity as outlined in Section 2.3. Insertion of (67) into the integration algorithm (17) yields the updates

$$\varepsilon^{\mathrm{p}}_{n+1} = \varepsilon^{\mathrm{p}}_n + \gamma n \quad \text{and} \quad A_{n+1} = A_n + \gamma \tag{68}$$

of the internal variables. The direction n can be identified with $n = (\varepsilon_{n+1} - \varepsilon^{\mathrm{p}}_n)/|\varepsilon_{n+1} - \varepsilon^{\mathrm{p}}_n|$. The multiplier γ is obtained by the Newton algorithm (23) that needs the derivatives

$$\left.\begin{aligned} W^h_{,\gamma} &= -E(|\varepsilon_{n+1} - \varepsilon^{\mathrm{p}}_n| - \gamma) + \zeta[1 - \exp(-A_{n+1}/\eta)] + hA_{n+1} + c, \\ W^h_{,\gamma\gamma} &= E + \zeta/\eta \exp(-A_{n+1}/\eta) + h. \end{aligned}\right\} \tag{69}$$

Note that $(69)_1$ represents the classical yield condition. If the solution point γ^* is found, exploitation of (24) and (26) yields the formulas for the stress and the tangent modulus

$$\sigma_{n+1} = E(\varepsilon_{n+1} - \varepsilon^{\mathrm{p}}_{n+1}) \quad \text{and} \quad \mathbb{C}_{n+1} = E - \frac{E^2}{E + \zeta/\eta \exp(-A_{n+1}/\eta) + h}. \tag{70}$$

These formulas only hold as long as the incremental stress potential $W(\varepsilon_{n+1})$ is convex in the sense of the convexity condition (34). Otherwise the convexification procedure needs to be performed as outlined in Section 4.

6.2. Numerical computation of the local convexified stress response

In this section we demonstrate the convexification analysis outlined in Section 4 by means of a numerical model problem. The set of material parameters governing the energy storage and dissipation functions is given in Table 4. The parameters are chosen such that they describe a combination of a saturation-type softening and a linear hardening response. The development of the internal variable B, plotted in Fig. 5, mirrors the combined softening/hardening behavior. After an initial softening governed by the parameters ζ and η the material hardens with the constant slope h. The problem is analyzed by a displacement-driven solution algorithm by linearly increasing the strain ε up to the final value $\varepsilon = 12$. The strain increment is set constant to $\Delta\varepsilon = 0.1$ for all subsequent computations.

Table 4
Set of material parameters

Elasticity modulus (E)	1.0000
Yield stress (c)	1.0000
Saturation softening (ζ)	−1.1353
Saturation intensity (η)	1.1182
Linear hardening (h)	0.0284

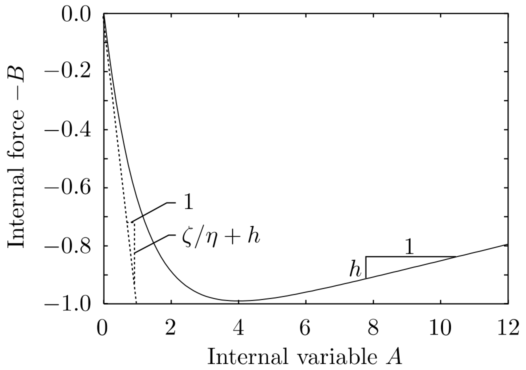

Fig. 5. Combination of softening/hardening response. The development of the internal variable B mirrors the combined softening/hardening response. After an initial softening governed by the parameters ζ and η the material hardens with the constant slope h.

6.2.1. Comparison of non-relaxed and relaxed response

Firstly, the non-relaxed stress–strain curve is computed based on the constitutive equations summarized in Section 6.1. As a consequence of the combined softening/hardening response visualized in Fig. 5 the stress response is non-convex. In Fig. 6a the non-convex stress–strain curve is plotted showing an initially linear elastic path until the elastic threshold $c = 1$ is reached. In the post-critical range the stress–strain curve reflects the prescribed strain-softening behavior depicted in Fig. 5. In order to detect the non-convex span of the incremental stress potential, within every time increment we perform the accompanying check of convexity outlined in Section 3.2. We start at the origin of Fig. 6 and proceed on the elastic loading branch. For $\varepsilon_{n+1} = 0.2$ the convexity condition (34) is not satisfied anymore. Only at $\varepsilon_{n+1} = 9.6$ the incremental stress potential is convex again in the sense of (34). The loss of convexity coincides with the non-uniqueness of the constitutive material behavior. Fig. 7 visualizes the shapes of the incremental stress potential W and the stress σ for the first two strain intervals $[0; 0.1]$ and $[0.1; 0.2]$. Fig. 7a and b illustrates the obvious non-convex shapes of the incremental stress potential W in the strain intervals considered. In the first strain interval $[0; 0.1]$ the actual strain $\varepsilon_{n+1} = 0.1$ lies in a convex span of the incremental stress

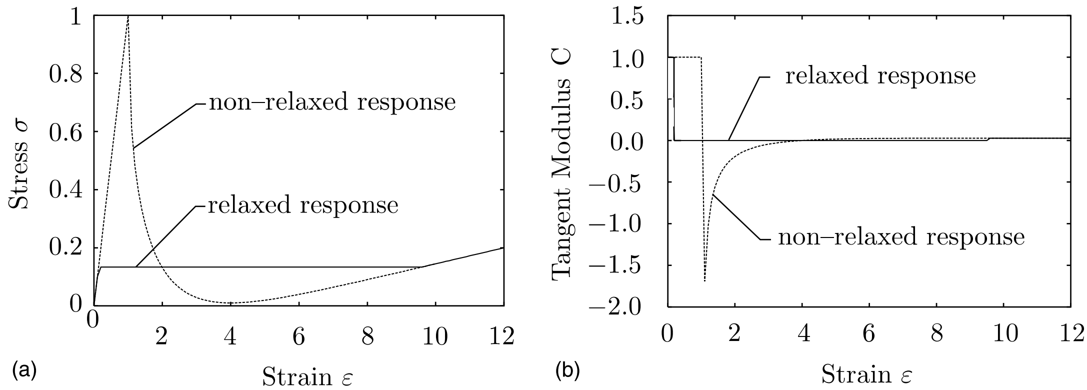

Fig. 6. Stress–strain curves. Visualization of the non-convex and convexified constitutive stress response. For the computation of the convexified solution within every interval $[\varepsilon_n; \varepsilon_{n+1}]$ the convexity of the incremental stress potential W is checked and, if necessary, replaced by its convexified counterpart.

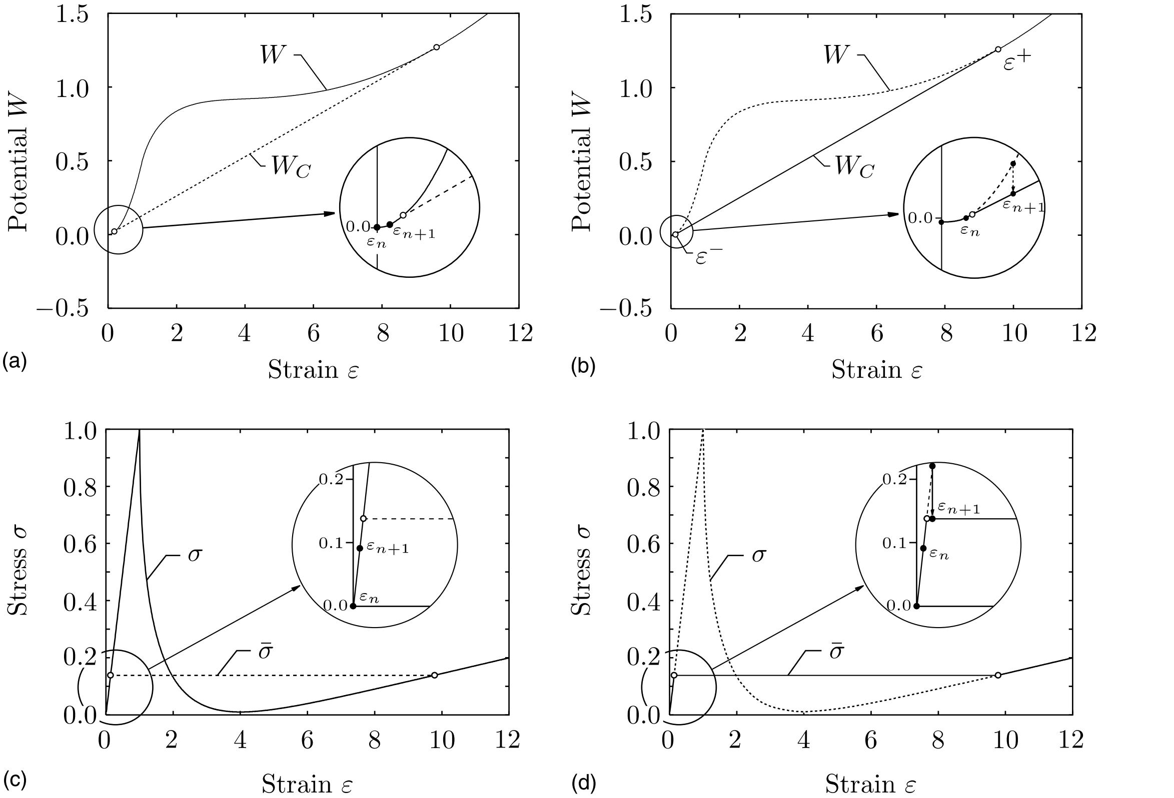

Fig. 7. Shape of the incremental stress potentials and stresses for the first two strain intervals: (a, b) incremental stress potentials W and (c, d) stresses σ for the time intervals $[0; 0.1]$ and $[0.1; 0.2]$, respectively. The magnified pictures reveal the convexity check and the convexification procedure if needed.

potential W (Fig. 7a). The associated incremental stress–strain diagram in Fig. 7c shows that the actual strain ε_{n+1} lies below the critical value of 0.1332. In the second strain interval $[0.1; 0.2]$ the potential W, evaluated at $\varepsilon_{n+1} = 0.2$, is non-convex (Fig. 7b) in the sense of convexity condition (34). Consequently, the stress state σ_{n+1} is unstable. Also, the associated stress strain diagram in Fig. 7d reveals that the actual strain ε_{n+1} lies above the critical stress for this increment. The magnified part in Fig. 7b shows the convexification procedure which essentially represents a fictitious projection of the actual strain onto the convex envelope W_C. Accordingly, in Fig. 7d the actual stress is projected onto the critical stress value. This stress response reflects the incremental snap-through behavior between the micro-strains ε^- and ε^+. As depicted in Fig. 6a, application of the convexification procedure of Section 4 leads to a stress–strain curve that shows a typical snap-through behavior between the phases (−) and (+). Fig. 6b compares the shapes of the tangent moduli in view of the non-relaxed and relaxed solutions. It turns out that the tangent moduli diverge considerably in the non-convex span $0.1332 < \varepsilon < 9.5788$.

6.2.2. Details of the convexification procedure

The goal of the subsequent discussion is to report on some details of the convexification analysis. As mentioned in Section 4.2 the solution of the minimization problem (34) is one crucial task in the context of the relaxation technique presented. Fig. 8a illustrates the obvious difficulty in view of the optimization

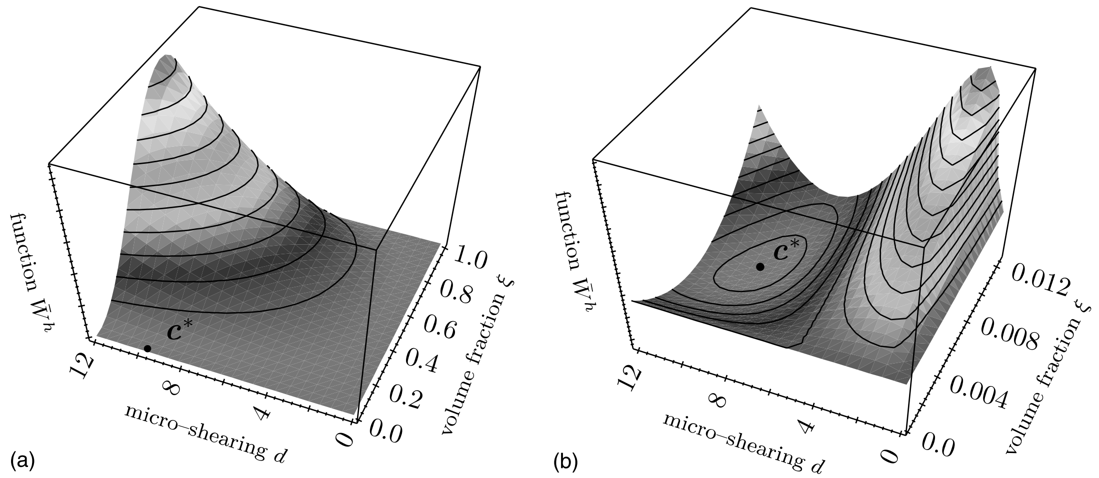

Fig. 8. Topography of function $\overline{W}^h$ (a) over the admissible domain $\mathscr{C}$ and (b) for the immediate neighborhood of the solution point $\boldsymbol{c}^*$. The figures visualize the non-convexity of the minimizing function $\overline{W}^h(\varepsilon_{n+1}, \boldsymbol{c})$.

problem. The topography shows the non-convex function $\overline{W}^h(\varepsilon_{n+1}, \boldsymbol{c})$ for the strain $\varepsilon_{n+1} = 0.2$ over the admissible domain $\mathscr{C}$. Here, the minimizing point $\boldsymbol{c}^* = [0.0071, 9.4456]^{\mathrm{T}}$ is close to the boundary $\xi = 0$. This minimum and its neighborhood is not at all distinctive compared to the whole domain shown. Clearly, if a standard Newton-type procedure was initialized somewhere within the domain the global minimum would not be found. Fig. 8b depicts the immediate surrounding of the minimum wanted. The solution is obtained by application of the strategy presented in Section 4.2. Fig. 9a and b plot the values of the volume fraction ξ and the micro-shearing d which determine the convexified solution $W_{\mathrm{C}}(\varepsilon_{n+1})$. Fig. 9a visualizes the development of the volume fraction ξ during the convexification analysis. From the initial value $\xi \approx 0$ the volume fraction increases linearly to its final value $\xi = 1$. Fig. 9b depicts the path of the micro-shearing d that represents the difference between the strains in the phases (+) and (−). During the convexification analysis the micro-shearing remains constant $d = 9.4456$. Fig. 10a reflects the evolution of the micro-strains which mark the initial and final points of the convex envelope, respectively. They remain constant for the whole non-convex span: $\varepsilon^+ = 9.5788$ and $\varepsilon^- = 0.1332$. In Fig. 10b the constant plastic strains $\varepsilon^{+^{\mathrm{p}}} = 9.4456$

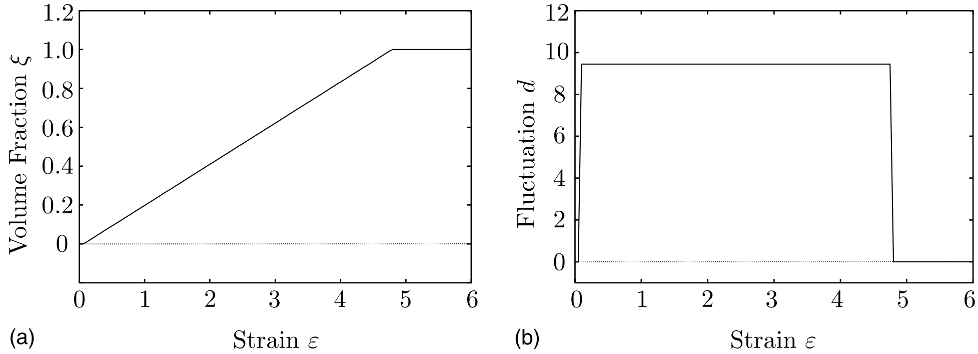

Fig. 9. Development of the volume fraction and the micro-shearing: (a) the volume fraction increases linearly from $\xi = 0$ to the final value $\xi = 1$ and (b) the constant discrete fluctuation $d = 9.4456$ determines the distance between the two phases (+) and (−).

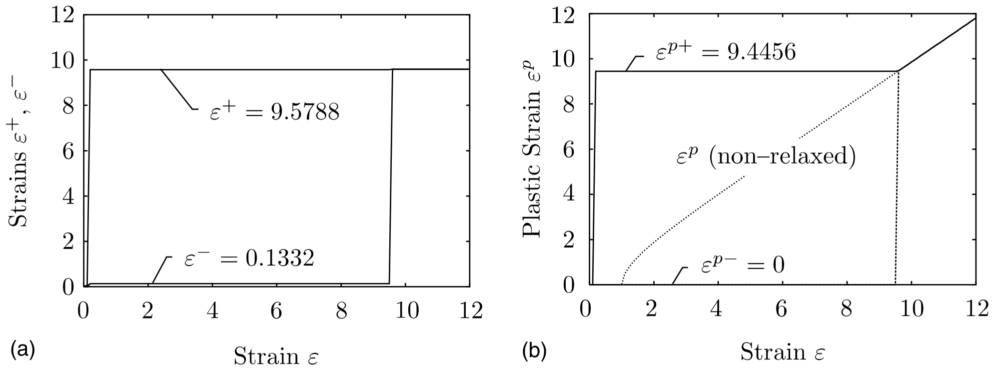

Fig. 10. Development of the total and plastic strains in the micro-phases. (a) The total strains ε^+, ε^- do not change during the convexification analysis. (b) Also the plastic micro-strains ε^{+^p}, ε^{-^p} remain constant in the non-convex span.

and $\varepsilon^{-^p} = 0$ are visualized. As a consequence, the elastic micro-strains $\varepsilon^{+^e} = \varepsilon^{-^e} = 0.1332$ are identical yielding the constant stress response $\sigma(\varepsilon^+) = \sigma(\varepsilon^-) = 0.1332$ for the whole non-convex range $0.132 < \varepsilon < 9.5788$.

6.3. Relaxation of a strain-softening elastic–plastic bar

In this section we consider the localization of a strain-softening elastic–plastic bar in tension. Main goal is the demonstration of the mesh-invariance of the proposed relaxation technique. We consider the strip depicted in Fig. 11 of length 1. The bar is fixed at its left boundary. In order to point out the mesh-dependence of the non-relaxed formulation we discretize the bar with two elements $\mathscr{B}_1$ and $\mathscr{B}_2$ for different lengths $\kappa = 0.2/0.4/0.6/0.8/1.0$. A localization of the homogeneous boundary-value problem is triggered by increasing the elastic threshold in the element $\mathscr{B}_1$ by 0.1%. The displacement $\tilde{u}$ of the right end is increased in constant increments $\Delta\tilde{u} = 0.1$. In dependence of the deformation D_{n+1} at $x = 1 - \kappa$ the constant strains

$$\varepsilon_{1,n+1} = D_{n+1}/(1-\kappa) \quad \text{and} \quad \varepsilon_{2,n+1} = (\tilde{u}_{n+1} - D_{n+1})/\kappa \tag{71}$$

in the elements $\mathscr{B}_1$ and $\mathscr{B}_2$ are defined. The displacement D_{n+1} is determined by means of the iterative Newton–Rapson update scheme

$$D_{n+1} \Leftarrow D_{n+1} - K^{-1} r \tag{72}$$

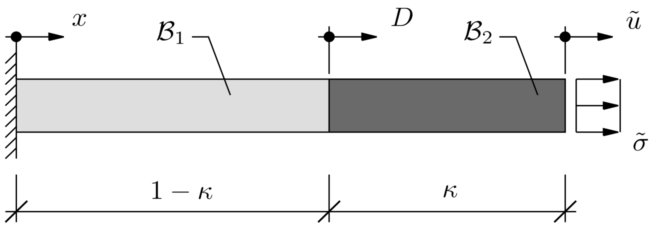

Fig. 11. Localization of a bar in tension. The test specimen under consideration consists of two parts: $\mathscr{B}_2$ with length κ and $\mathscr{B}_1$ with length $1-\kappa$. In $\mathscr{B}_1$ the yield stress c is increased by 0.1%.

in terms of the residual and the tangent

$$r := \check{\sigma}_{n+1}(\varepsilon_{1,n+1}) - \check{\sigma}_{n+1}(\varepsilon_{2,n+1}), \qquad K := \check{\mathbb{C}}_{n+1}(\varepsilon_{1,n+1})/(1-\kappa) + \check{\mathbb{C}}_{n+1}(\varepsilon_{2,n+1})/\kappa, \tag{73}$$

where the residual represents the equilibrium condition of the bar. The reverse hat ($\check{\circ}$) indicates that either the convex or the convexified quantity is used. The iteration is terminated for $|r(D^*_{n+1})| < \text{tol}$ where D^*_{n+1} is considered to be the solution of (72). Fig. 12a depicts the stress–displacement curves for the different discretizations mentioned above.

We start at the origin of the diagram and proceed on the elastic loading branch. At the peak of the displacement curves in Fig. 12a we observe a loss of global structural stability documented by a change of sign of the tangent K. After the peak the element $\mathscr{B}_1$ switches onto a post-critical path while the element $\mathscr{B}_2$ switches back to the elastic unloading path. The non-convex analysis yields the spectrum of equilibrium paths in Fig. 12a. They document the well-known strong mesh-dependence of the non-objective post-critical analysis. These post-critical results are physically meaningless. The crucial mesh-dependence was pointed out for example by Crisfield (1982), de Borst (1987) and Belytschko et al. (1988). The ill-posed boundary-value problem can be transformed into a well-posed one by means of the relaxation method suggested in Section 4. The relaxed analysis yields an identical result for all mesh densities. The mesh-invariant post-critical equilibrium path is documented in Fig. 12b. Fig. 13 shows the course of the displacement $u(x)$ for the non-relaxed and the relaxed stress responses at $\tilde{u} = 1.0$ for three different discretizations $\kappa = 0.25/0.5/0.75$. In Fig. 13a the displacement field of the non-convex stress response is plotted which documents the dependence on the discretizations. Application of the two-phase relaxation analysis yields the displacement fields given in Fig. 13b. The zigzag lines represent minimizing sequences which arise because of the phase-decay of the unstable homogeneous deformation state ε_{n+1} into the micro-strains ε^+ and ε^-. Note that the exact course of the displacement in the non-convex domain $\mathscr{B}_2$ cannot be determined, but its probability in terms of the volume fractions ξ, $1-\xi$ of the micro-phases (+) and (−), respectively. As a consequence, an effective mesh-invariant displacement field (dotted line) can be determined. Fig. 14 visualizes the micro-structure development in the localized zone. Due to the loss of convexity two micro-phases (+) and (−) occur in the localized elements. For the discretizations $\kappa = 0.25/0.5/0.75$ the volume fractions of the white phase (+) are $\xi \approx 0.36/0.18/0.13$. As a consequence the global distributions of the two strains ε^+ and ε^- are identical. This leads to the objective load–displacement curve.

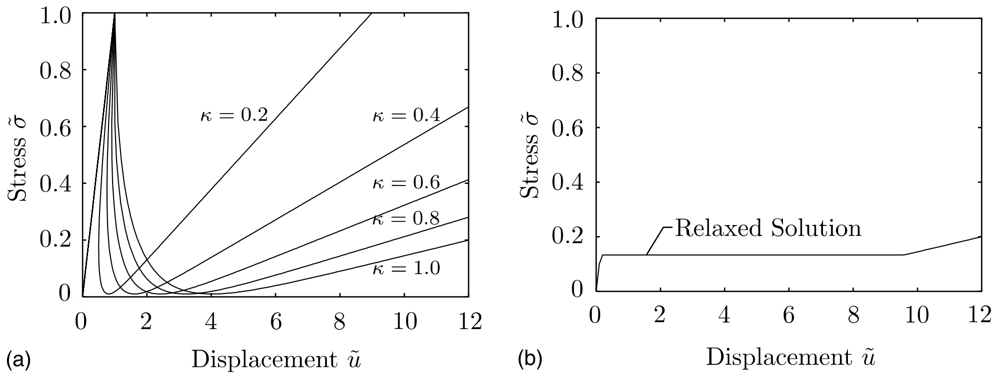

Fig. 12. Global stress–strain curves of imperfect test specimen: (a) Visualization of the length-dependent stress response for different choices κ within the standard formulation and (b) invariant solution due to the convexification analysis.

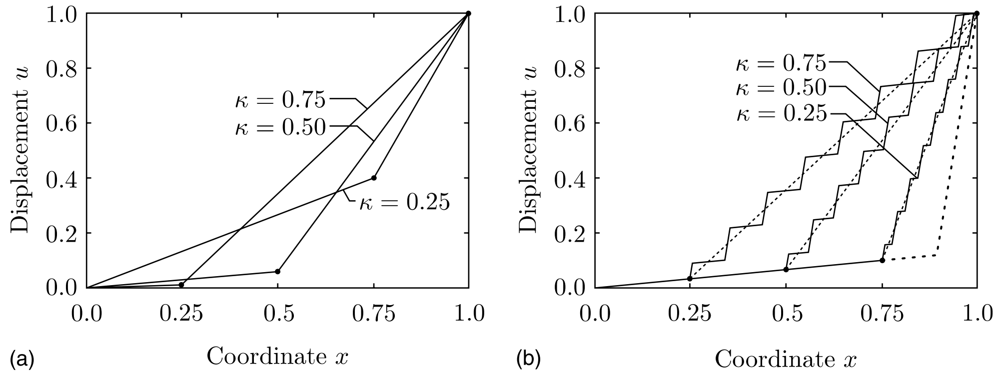

Fig. 13. Course of the displacement over the length of the bar at $\tilde{u} = 1.0$. (a) Non-relaxed response: due to the non-convexity of the stress potential the displacement field $u(x)$ differs for different discretizations κ yielding a mesh-dependent stress response. (b) Relaxed response: the phase decay into the micro-strains ε^+ and ε^- with the volume fractions ξ, $1 - \xi$ leads to the effective mesh-invariant displacement field $(\cdots)$ ensuring an objective stress response.

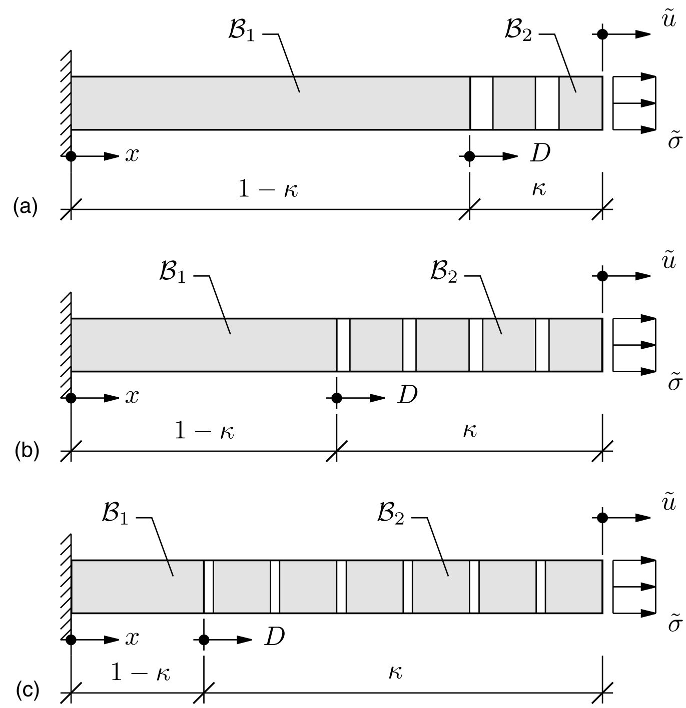

Fig. 14. Micro-strcucture development in localized zone. Due to the loss of convexity two micro-phases (+) and (−) occur in the localized elements. For the discretizations $\kappa = 0.25/0.5/0.75$ the volume fractions of the white phase (+) are $\xi \approx 0.36/0.18/0.13$. As a consequence the global distribution of the two strains ε^+ and ε^- is identical. This leads to the objective load–displacement curve.

7. Conclusion

We proposed a new approach to the treatment of material instabilities in a strain-softening elastic–plastic bar based on energy minimization principles associated with micro-structure developments. At first we outlined an incremental variational formulation of the local constitutive response that includes the derivation of a quasi-hyperelastic stress potential from a local constitutive minimization problem with respect to the internal variables. In analogy to treatments in finite elasticity the existence of this variational formulation allows for the definition of the material stability of a homogeneous solid based on the convexity of the incremental stress potential. The micro-phases arising are resolved by the relaxation of the non-convex incremental stress potential. Here, the key point is the convexification of the incremental stress potential that requires the solution of a local minimization problem for a relaxed stress potential with respect to two variables representing a volume fraction and an intensity of the micro-bifurcation. The concept of the two-phase relaxation analysis is summarized in Table 3. The performance of the energy relaxation method proposed was demonstrated by the localization of an elastic–plastic bar that reports on the mesh-independence of the result.

Acknowledgements

Support for this research was provided by the Deutsche Forschungsgemeinschaft (DFG) under grant SFB 404/C11. The authors are grateful for stimulating discussions with Alexander Mielke.

Appendix A. Derivatives for the convexification analysis

The first and second derivatives of the minimizing function $\overline{W}^h$ needed in the above outlined convexification analysis for the Newton-iteration (44) have the form

$$\left.\begin{aligned}
\overline{W}^h_{,d} &= \xi(1-\xi)[\sigma(\varepsilon^+) - \sigma(\varepsilon^-)],\\
\overline{W}^h_{,\xi} &= W(\varepsilon^+) - W(\varepsilon^-) - d[\xi\sigma(\varepsilon^+) + (1-\xi)\sigma(\varepsilon^-)],\\
\overline{W}^h_{,\xi\xi} &= 2d[\sigma(\varepsilon^-) - \sigma(\varepsilon^+)] + d^2[\xi\mathbb{C}(\varepsilon^+) + (1-\xi)\mathbb{C}(\varepsilon^-)],\\
\overline{W}^h_{,dd} &= \xi(1-\xi)[\xi\mathbb{C}(\varepsilon^-) + (1-\xi)\mathbb{C}(\varepsilon^+)],\\
\overline{W}^h_{,\xi d} &= (1-2\xi)[\sigma(\varepsilon^+) - \sigma(\varepsilon^-)] + d\xi(1-\xi)[\mathbb{C}(\varepsilon^-) - \mathbb{C}(\varepsilon^+)].
\end{aligned}\right\} \tag{A.1}$$

In order to determine the relaxed stress and the relaxed tangent modulus defined in (47) and (50) we need the derivatives

$$\left.\begin{aligned}
\overline{W}^h_{,\varepsilon} &= \xi\sigma(\varepsilon^+) + (1-\xi)\sigma(\varepsilon^-),\\
\overline{W}^h_{,\varepsilon\varepsilon} &= \xi\mathbb{C}(\varepsilon^+) + (1-\xi)\mathbb{C}(\varepsilon^-),\\
\overline{W}^h_{,\varepsilon\xi} &= \sigma(\varepsilon^+) - \sigma(\varepsilon^-) - d[\xi\mathbb{C}(\varepsilon^+) + (1-\xi)\mathbb{C}(\varepsilon^-)],\\
\overline{W}^h_{,\varepsilon d} &= \xi(1-\xi)[\mathbb{C}(\varepsilon^+) - \mathbb{C}(\varepsilon^-)]
\end{aligned}\right\} \tag{A.2}$$

of the minimizing function $\overline{W}^h$. Note that the pure derivatives with respect to the strain ε represent the volume averages of the stresses and tangent moduli in the phases (+) and (−).

References

Bažant, Z.P., Lin, F.B., 1988. Non-local yield limit degradation. International Journal for Numerical Methods in Engineering 26, 1805–1823.

Belytschko, T., Fish, J., Engelmann, B.E., 1988. A finite element with embedded localization zones. Computer Methods in Applied Mechanics and Engineering 70, 59–89.

Biot, M.A., 1965. Mechanics of Incremental Deformation. John Wiley, New York.

de Borst, R., 1987. Computation of post-bifurcation and post-failure behaviour of strain-softening solids. Computers and Structures 25, 211–224.
de Borst, R., Sluys, L.J., 1991. Localization in a Cosserat continuum under static and dynamic loading. Computer Methods in Applied Mechanics and Engineering 90, 805–827.
Carstensen, C., Roubíček, T., 2000. Numerical approximation of Young measures in non-convex variational problems. Numerische Mathematik 84, 395–415.
Ciarlet, P.G., 1988. Mathematical Elasticity. Elsevier Science Publishers, Amsterdam.
Crisfield, M.A., 1982. Local instabilities in the non-linear analysis of reinforced concrete beams and slabs. Proceedings of the Institution of Civil Engineers 73, 135–145.
Dacorogna, B., 1989. Direct Methods in the Calculus of Variations. Springer-Verlag, Berlin.
DeGiorgi, E., 1968. Teoremi di semicontinuità nel calcolo delle variazioni. Istituto Nazionale di Alta Matematica, Roma.
Germain, P., 1973. Cours de Mécanique des Milieux Continus. Masson et Cie, Paris.
Halphen, B., Nguyen, Q.S., 1975. Sur les Matéraux Standards Généralisés. Journal de Mécanique 40, 39–63.
Hill, R., 1962. Acceleration waves in solids. Journal of the Mechanics and Physics of Solids 6, 1–16.
Krawietz, A., 1986. Materialtheorie: Mathematische Beschreibung des phänomenologischen thermomechanischen Verhaltens. Springer-Verlag, Berlin.
Larsson, R., Runesson, K., Ottosen, N.S., 1993. Discontinuous displacement approximation for capturing plastic localization. International Journal for Numerical Methods in Engineering 36, 2087–2105.
Marsden, J.E., Hughes, T.J.R., 1994. Mathematical Foundations of Elasticity. Dover Publications Inc, New York.
Martin, J.B., 1975. Plasticity: Fundamentals and General Results. MIT press, Cambridge, MA.
Maugin, G.A., 1992. The Thermodynamics of Plasticity and Fracture. Cambridge University Press, Cambridge.
Miehe, C., 2002. Strain-driven homogenization of inelastic micro-structures and composites based on an incremental variational formulation. International Journal of Numerical Methods in Engineering 55 (11), 1285–1322.
Miehe, C., Schotte, J., Lambrecht, M., 2002. Homogenization of inelastic materials at finite strains based on incremental minimization principles. Journal of the Mechanics and Physics of Solids 50, 2123–2167.
Miehe, C., Schröder, J., 1994. Post-critical discontinuous localization analysis of small-strain softening elastoplastic solids. Archive of Applied Mechanics 64, 267–285.
Mühlhaus, H.B. (Ed.), 1995. Continuum Models for Material with Microstructure. John Wiley, Chichester.
Mühlhaus, H.B., Aifantis, E.C., 1991. A variational principle for gradient plasticity. International Journal of Solids and Structures 28, 845–858.
Müller, S., 1998. Variational models for microstructure and phase transitions. In: Bethuel, F., Huisken, G., Müller, S., Steffen, K., Hildebrandt, S., Struwe, M. (Eds.), Calculus of Variations and Geometric Evolution Problems. Springer Lecture Notes in Mathematics. Springer-Verlag, Berlin.
Nadai, A., 1950. Theory of Flow and Fracture of Solids, vol. I. McGraw-Hill, New-York.
Needleman, A., 1988. Material rate dependence and mesh sensitivity in localization problems. Computer Methods in Applied Mechanics and Engineering 67, 69–85.
Nguyen, Q.S., 2000. Stability and Nonlinear Solid Mechanics. John Wiley, Chichester.
Ortiz, M., Repetto, E.a., 1999. Nonconvex energy minimization and dislocation structure in ductile single crystals. Journal of the Mechanics and Physics of Solids 47, 397–462.
Rice, J.R., 1976. The localization of plastic deformation. In: Koiter, W.T. (Ed.), Theoretical and Applied Mechanics. North-Holland, Amsterdam, pp. 207–220.
Rockafellar, R.T., 1970. Convex Analysis. Princeton University Press, Princeton.
Rowlinson, J.S., 1958. The properties of real gases. In: Flügge, S. (Ed.), Handbuch der Physik Band XII. Springer-Verlag, Berlin.
Runesson, K., Larsson, R., 1993. Properties of incremental solutions for a dissipative material–Potential energy and stability. Journal of Engineering Mechanics, ASCE 119, 647–666.
Šilhavý, M., 1997. The Mechanics and Thermodynamics of Continuous Media. Springer-Verlag, Berlin.
Simó, J.C., Oliver, J., Armero, G., 1993. An analysis of strong discontinuities induced by strain-softening. Computational Mechanics 12, 277–296.
Thomas, T.Y., 1961. Plastic Flow and Fracture in Solids. Academic Press, London.
Tonelli, L., 1921. Fondamenti di calcolo delle variazioni. Zanichelli, Bologna.
Vardoulakis, I., 1977. Scherfugenbildung in Sandkörpern als Verzweigungsproblem, Veröffentlichungen des Instituts für Bodenmechanik und Felsmechanik der Universität Karlsruhe, Heft 70, Universität Karlsruhe.
Young, L.C., 1921. Lectures on the Calculus of Variations and Optimal Control Theory. Saunders, London.
Ziegler, H., 1963. Some extremum principles in irreversible thermodynamics with application to continuum mechanics. In: Sneddon, I.N., Hill, R. (Eds.), Progress in Solid Mechanics, vol. 4. North-Holland Publishing Company, Amsterdam.